Nonlinear Controller for Automotive Thermal Management Systems

P. Setlur, J. Wagner, D. Dawson, and J. Chen
Automotive Research Laboratory
Fluor Daniel Engineering Innovation Building, Clemson University
Clemson, South Carolina 29634
voice: (864) 656-7376; fax: (864) 656-4435
email: jwagner@clemson.edu

Abstract

The functionality of gasoline and diesel engine thermal management systems can be enhanced through the introduction of a smart thermostat valve and variable speed water pump. A nonlinear tracking controller is presented in this paper for advanced thermal management systems applicable to ground vehicles. Specifically, the controller is designed to ensure that the engine temperature follows a desired temperature trajectory which may be prescribed based on operating conditions. Further, the heat rejected from the system at the radiator is controlled by adjusting the radiator fan's speed. The controller ensures that the engine temperature tracking error is asymptotically forced to zero while compensating for the unmeasurable heat input from the engine's combustion process. Representative numerical results are presented to illustrate the performance of the proposed controller.

1 Introduction

Passenger and commercial ground vehicles use a variety of sensors, actuators, and on-board controllers to monitor and regulate the operation of the internal combustion engine, transmission, chassis, and safety subsystems. These mechatronic system components permit improved vehicle performance, fuel economy, tailpipe emissions, and occupant safety [2]. For example, the spark ignition engine often features electronic throttle control, fuel injectors, exhaust gas recirculation valve, and electronic spark to control the combustion process (e.g., [3]). However, the engine cooling system components and thermal control strategy have not been significantly redesigned to realize greater engine thermal efficiency [14]. Thus, an opportunity exists to introduce a smart thermostat valve and electric water pump to enhance the fluid flow regulation process [16].

The traditional automotive cooling system components include a wax based thermostat valve and crankshaft driven water pump. However, a servo-motor valve and pump can better regulate the coolant fluid flow in the engine to realize fuel economy gains and emission reductions. Advanced thermal system technologies can provide 1%-3% fuel economy improvements through lower parasitic losses, higher operating temperatures, reduced component temperature fluctuations, lowered emissions, and alternative engine block monitoring temperatures [18]. As a side note, thermal management system concepts can be applied to other systems including power electronic circuits.

In high density computer installations, water cooling may provide an attractive alternative to the commonplace air cooling which relies on local room air conditioners.

Automotive thermal management system research has been pursued for two decades. Xu *et al.*, [19], [20] developed, simulated, and tested a control scheme for various components of a heavy truck diesel engine cooling system with an accompanying model. Xu *et al.* introduced a computer controlled fan clutch, variable speed pump, and a modified thermostat with limited controllability. Einaudi and Mortara [6] proposed a PID controlled vacuum actuated mixing valve for higher engine temperature levels. Similar research was pursued by Kenny *et al.* [9] with a stepper motor driven butterfly valve under engine control unit (ECU) supervision. A servo-motor pump and butterfly valve were studied by Couetouse and Gentile [4] to regulate cylinder head temperature for reduced fuel consumption and enhanced passenger comfort. Recently, electric pumps have been proposed [1], [8] to reduce engine internal parasitic power for greater thermal efficiency, resulting in the reduction in component weight, and improved emissions through consistent cylinder temperature control. Melzer *et al.* [10] proposed a comprehensive thermal management system to meet an engine's cooling system needs; however, the controller structure was not fully explored. Gunter and Nalim [7] compared the transient performance of electrically heated wax-based thermostat valves with a conventional component. Wagner *et al.* [15] presented multi-node thermal models to estimate the temperature of in-cylinder and cylinder head components for air and liquid cooled internal combustion engines. A mechatronic thermostat valve was designed and modeled by Wagner *et al.* [17] for the continual on-line regulation of the coolant flow using in-cylinder temperature estimates.

In this paper, a Lyapunov-based nonlinear control algorithm will be designed for precise temperature tracking during transient operations. To compensate for the unmeasurable heat input, a recent idea found in [11] and [12] is modified to develop a tracking controller in the presence of an unknown disturbance. The controller ensures global asymptotic engine temperature tracking. The control design only imposes boundedness and smoothness restrictions on the unmeasurable disturbance signals. Representative numerical results are presented and discussed to investigate the enhanced engine thermal management system control architecture. The paper is organized as follows. In Section 2, the control objectives are stated. The system model for the thermal system is presented followed by the open-loop tracking dynamics, in Section 3. In Section 4, the design of the proposed tracking controller is presented along with the corresponding closed-loop error system. The stability analysis is given in Section 5, followed by representative numerical simulation results in Section 6. Concluding remarks are presented in Section 7.

2 Problem Statement

The control objective for an advanced automotive thermal management system is twofold. First, it is necessary to ensure that engine temperature follows a desired temperature profile while compensating for the unmeasurable combustion process heat input. To achieve this goal, the coolant flow rate must be controlled along with an auxiliary heating element located in the coolant circuit flowpath just before the engine block. Second, to ensure that the engine temperature remains controllable, and that radiator temperature remains bounded, the radiator fan speed must be varied to control the heat dissipated at the radiator.

3 Dynamic Model Development

3.1 System Description

The automotive thermal management system consists of the engine, which produces heat as a result of fuel combustion in its cylinders, the radiator, the thermostat valve, and the pump as shown in Figure 1. To avoid overheating the engine, coolant is forced through jackets in the engine by means of the water pump. The coolant transfers heat to the radiator which is finally dissipated to the surrounding ambient environment. Additionally, the system may sport a heater coil (*i.e.*, quick heat coil) to rapidly raise the engine's operating temperature in colder temperature zones.

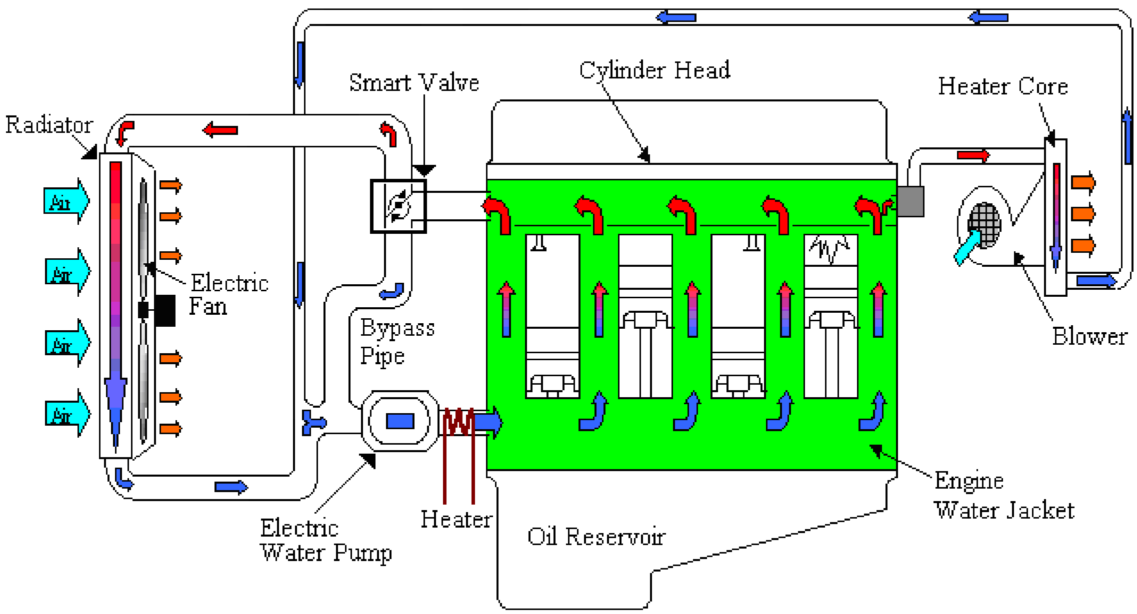

Figure 1: Advanced spark ignition engine thermal management system architecture

To initiate the model-based controller design process, a reduced order dynamic model shall be established for the system which permits real-time applications. A two-node lumped parameter thermal model is presented to describe the transient phenomena of the thermal network shown in Figure 2. Simply put, the system corresponds to a variable resistive element heating the coolant, a radiator with adjustable heat rejection, smart thermostat valve and a variable speed water pump. The cooling system has been divided into two nodes (*viz.*, engine and radiator). The smart valve controls the quantity of coolant that flows through the radiator. Based on the various coolant flow paths, heat energy is exchanged between the two nodes.

3.2 Model Formulation

The thermal dynamics for the two nodes in the vehicle thermal management system architecture may be expressed as

$$C_e \dot{T}_e = -c_{pc} \dot{m}_{cool} \left(T_e - T_j \right) + Q_{in} \left(t \right) + Q_H \left(t \right) \tag{1}$$

$$C_r \dot{T}_r = c_{pc} H \dot{m}_{cool} \left(T_e - T_r \right) - Q_{out} \left(t \right) \tag{2}$$

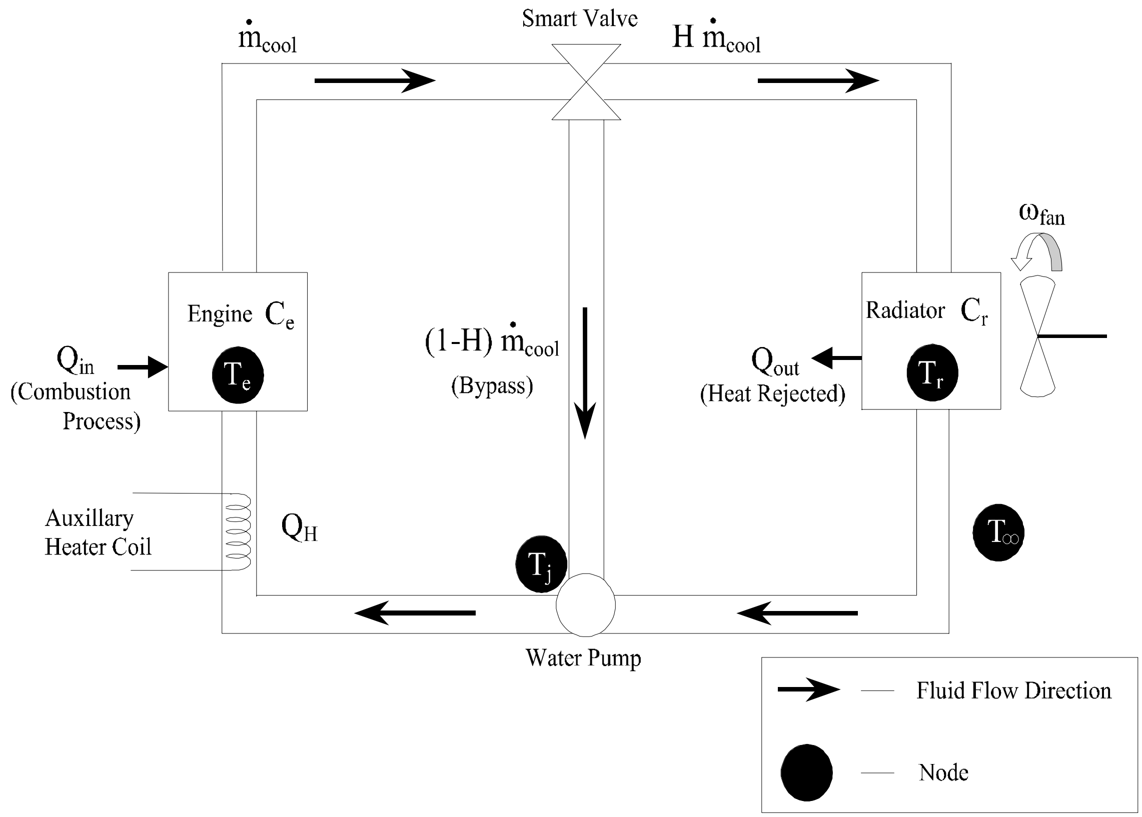

Figure 2: Reduced order engine thermal management system schematic

where $T_e(t)$, $T_r(t) \in \mathbb{R}^1$ denote the temperature of the coolant at the engine and radiator nodes, respectively, C_e, $C_r \in \mathbb{R}^1$denote the thermal capacitance constants associated with the engine and radiator coolant nodes, respectively. $\dot{m}_{cool}(t) \in \mathbb{R}^1$ is the mass flow rate of the coolant at the engine that can be controlled by the speed of the pump. The control input, $H(t)$, represents the smart valve position satisfying $0 \leq H(t) \leq 1$; note that $H(t) = 0\,(1)$ corresponds to a fully closed(open) valve position. The positive constant $c_{pc} \in \mathbb{R}^1$ is the specific heat of the coolant. The signal $T_j(t) \in \mathbb{R}^1$, denoting the temperature of the coolant at the junction, is algebraically related to the engine and the radiator temperature by

$$T_j = (1 - H)\,T_e + HT_r. \tag{3}$$

The heat energy entering the system from the combustion process at the engine node is denoted by the unmeasurable variable $Q_{in}(t) \in \mathbb{R}^1$. Additionally, the control input $Q_H(t) \in \mathbb{R}^1$ may also be applied to increase the engine's operating temperature. At the radiator, the heat energy lost to the ambience is $Q_{out}(t)$ which can be explicitly expressed as

$$Q_{out} = Q_0(t) + \kappa\,(T_r - T_\infty)\,\omega_{fan} \tag{4}$$

where $Q_0(t) \in \mathbb{R}^1$ represents the unmeasurable heat lost at the radiator due to uncontrollable air flow through the radiator, $T_\infty \in \mathbb{R}^1$ denotes the ambient temperature, the control input denoted by $\omega_{fan}(t) \in \mathbb{R}^1$ is the speed of the radiator fan, and the positive constant $\kappa \in \mathbb{R}^1$ is defined as

$$\kappa = \varepsilon \rho_a A r c_{pa} \tag{5}$$

where $\varepsilon \in \mathbb{R}^1$ is the heat exchanger efficiency, $\rho_a \in \mathbb{R}^1$ is air density, $A \in \mathbb{R}^1$ denotes the area of heat exchanger exposed to the radiator fan, $r \in \mathbb{R}^1$ is the nominal radius of the fan, and $c_{pa} \in \mathbb{R}^1$ is the specific heat of air. In this model development, the heat capacity rate of air has been assumed to be smaller than the coolant (*i.e.*, $\dot{m}_a c_{pa} < \dot{m}_{cool} c_{pc}$).

Remark 1 *It is assumed that the function $Q_{in}(t)$ and its first two time derivatives remain bounded at all time, such that $Q_{in}(t), \dot{Q}_{in}(t), \ddot{Q}_{in}(t) \in \mathcal{L}_\infty$.*

Remark 2 *From the physics of the problem, it is clear that the signals $Q_{in}(t)$ and $Q_0(t)$ always remain positive (i.e., $Q_{in}, Q_0 \geq 0$).*

Remark 3 *In the analysis, it is assumed that the ambient temperature, $T_\infty \in \mathbb{R}^1$ is constant and satisfies*

$$T_r - T_\infty \geq \varepsilon_0 \qquad \forall t \geq 0 \tag{6}$$

where $\varepsilon_0 \in \mathbb{R}^1$ is some positive constant, and $T_r(t)$ was introduced in equation (2). It is also assumed that $T_e(0) > T_r(0)$ to facilitate the boundedness of signal argument used in the subsequent stability analysis.

3.3 Open-Loop Error System Development

To quantify the control objectives, the filtered tracking error signal, denoted by $s(t) \in \mathbb{R}^1$, and an auxiliary signal $y(t) \in \mathbb{R}^1$, are defined as

$$s = \dot{e} + \beta e \tag{7}$$

$$y = \frac{1}{\eta} + \varepsilon_1 \tag{8}$$

where $\beta \in \mathbb{R}^1$ represents a positive control gain, $\varepsilon_1 \in \mathbb{R}^1$ is a positive constant for analysis, the engine temperature tracking error signal, $e(t) \in \Re^1$ is defined as

$$e = T_{ed} - T_e, \tag{9}$$

and $T_{ed}(t) \in \mathbb{R}^1$ is the desired trajectory for the engine temperature. The auxiliary signal $\eta(t) \in \mathbb{R}^1$ introduced in equation (8) is defined as

$$\eta = T_e - T_r. \tag{10}$$

After taking the first time derivative of equation (7), and then multiplying both sides of the resulting equation by C_e, and then substituting the system dynamics given by equations (1) through (3), the open loop error system for the engine temperature control system can be written as

$$C_e \dot{s} = -e + N(T_e, \dot{T}_e, t) - \dot{u}_1 \tag{11}$$

where the unknown disturbance function, denoted by $N(T_e, \dot{T}_e, t) \in \mathbb{R}^1$, is defined as

$$N(T_e, \dot{T}_e, t) \triangleq C_e \ddot{T}_{ed} - \dot{Q}_{in} + C_e \beta \dot{e} + e \tag{12}$$

and the auxiliary control input $u_1(t) \in \mathbb{R}^1$ is defined as

$$u_1 = Q_H - u_3 (T_e - T_r) \tag{13}$$

where the control input $u_3(t) \in \mathbb{R}^1$ is defined by

$$u_3 = c_{pc} H \dot{m}_{cool} \tag{14}$$

Remark 4 *It is assumed that the desired engine temperature profile is always bounded and is chosen so that its first three time derivatives remain bounded at all times (i.e.,* $T_{ed}(t)$*,* $\dot{T}_{ed}(t)$*,* $\ddot{T}_{ed}(t)$*,* $\dddot{T}_{ed}(t) \in \mathcal{L}_\infty$*).*

Remark 5 *Based on the definition of* $s(t)$ *given in equation (7), standard arguments [5] can be used to prove that: (i) if* $s(t) \in \mathcal{L}_\infty$*, then* $e(t)$*,* $\dot{e}(t) \in \mathcal{L}_\infty$*, and (ii) if* $s(t)$ *is asymptotically regulated, then* $e(t)$*,* $\dot{e}(t)$ *are asymptotically regulated.*

Remark 6 *Based on the definition of* $y(t)$ *given in equations (8), it is easy to see that if* $y(t) \in \mathcal{L}_\infty$*, then* $\eta(t) \neq 0$*. Further, if* $y(t) \in \mathcal{L}_\infty$*, then it is also clear from equations (8) and (10) that if* $T_e(0) > T_r(0)$ *(See Remark 3), then* $T_e(t) > T_r(t), \forall t \geq 0$*.*

To ensure that all signals remain bounded, we design the control input $\omega_{fan}(t)$ for the dynamics of the auxiliary signal $y(t)$ introduced in (8). To this end, the time derivative of $y(t)$ given in equation (8) is taken. After using equation (10) and its first time derivative, the system equations given by equations (1), (2), and (3) are substituted to obtain

$$\begin{aligned} \dot{y} \;=\; & \left(\frac{1}{C_e} + \frac{1}{C_r}\right) u_3 (y + \varepsilon_1) - \frac{1}{C_e}\left(Q_{in} + Q_H\right)(y + \varepsilon_1)^2 \\ & - \frac{1}{C_r} Q_0(t)(y + \varepsilon_1)^2 - \frac{1}{C_r}(T_r - T_\infty) u_2 (y + \varepsilon_1)^2 \end{aligned} \tag{15}$$

where the control input $u_2(t) \in \mathbb{R}^1$ is defined as $u_2 = \kappa \omega_{fan}$.

Remark 7 *It may seem that the control problem has three control inputs,* $Q_H(t)$*,* $u_3(t)$ *and* $u_2(t)$*, and only one tracking objective. However, it is noted here that the three control inputs are unipolar. Hence, a commutation strategy is designed to implement the bipolar control input* $u_1(t)$*, as*

$$u_3 = \left\{ \begin{array}{ll} \dfrac{-u_1}{\eta} & \forall u_1 \in (-\infty, 0] \\ 0 & \forall u_1 \in (0, \infty) \end{array} \right\} \tag{16}$$

$$Q_H = \left\{ \begin{array}{ll} 0 & \forall u_1 \in (-\infty, 0] \\ u_1 & \forall u_1 \in (0, \infty) \end{array} \right\} \tag{17}$$

From these definitions, it is clear that if $u_1(t) \in \mathcal{L}_\infty$ *and if* $\eta(t) \neq 0, \forall t \geq 0$*, then* $Q_H(t)$*,* $u_3(t) \in \mathcal{L}_\infty$*. The choice of* $H(t)$ *and* $\dot{m}_{cool}(t)$ *to produce the required control input defined in equation (16) can be determined based on energy optimization issues. Further, this allows* $u_3(t)$ *to approach zero without stagnation of the coolant. The unipolar control input* $u_2(t)$*, introduced in equation (15), will be designed to ensure that all signals remain bounded in the closed loop system.*

4 Control Development

In light of the error definitions in Section 3.3, the control objective is to design a controller that forces the engine temperature tracking error signals, $s(t)$ and $e(t)$, to zero while compensating for the unknown disturbance $N(T_e, \dot{T}_e, t)$. It is assumed that the signals $T_e(t)$ and $T_r(t)$ are available for measurement by thermocouples or thermistors. It is also assumed that the radiator constants comprised in κ are known along with the specific heat of the coolant, c_{pc}.

4.1 Control Formulation

Based on the subsequent stability analysis, the following *continuous* control law[1] is proposed to achieve the first control objective

$$u_1(t) = (k_s + \beta)\, e(t) - (k_s + \beta)\, e(t_0) + \int_{t_0}^{t} [\beta\, (k_s + \beta)\, e(\tau) + \rho \mathrm{sgn}(e(\tau))]\, d\tau \tag{18}$$

where k_s, $\rho \in \mathbb{R}^1$ are positive control gains, t_0 is the initial time, $\mathrm{sgn}(\cdot)$ denotes the standard signum function, and $\beta \in \mathbb{R}^1$ was previously introduced in equation (7). Based on the structure of the commutation strategy given in equation (16), the control input $u_2(t)$ is designed as

$$u_2 = K_\eta u_3^2 + K_e \tag{19}$$

where control gains K_η, $K_e \in \mathbb{R}^1$ are positive constants. The control law in equation (18) ensures asymptotic tracking for the engine temperature provided the control gain ρ is chosen sufficiently large relative to a *reference trajectory-based* bound. The proof of this result is presented in the following two subsections. In particular, the closed-loop error system is first developed under the proposed control law. Its stability is then analyzed using a Lyapunov-based argument.

4.2 Closed-Loop Error System Development

After taking the time derivative of equation (18), the following system is obtained

$$\dot{u}_1 = (k_s + \beta)s + \rho \mathrm{sgn}(e) \tag{20}$$

upon use of equation (7). After substituting equations (20) into (11), the closed loop system may be rewritten as

$$C_e \dot{s} = -e - (k_s + \beta)s - \rho \mathrm{sgn}(e) + N(T_e, \dot{T}_e, t). \tag{21}$$

In order to write the closed loop error system in a more convenient form, $\tilde{N}(t) \in \mathbb{R}^1$ is defined as

$$\tilde{N} \triangleq N - N_d \tag{22}$$

where the signal $N_d(t) \in \mathbb{R}^1$ is defined as

$$N_d(t) \triangleq N(T_{ed}, \dot{T}_{ed}, t) \tag{23}$$

where $N(\cdot)$ was defined in equation (12). Using these definitions, the closed loop error system given in equation (21) may be rewritten as

$$C_e \dot{s} = -e - (k_s + \beta)s - \rho \mathrm{sgn}(e) + \tilde{N}(T_e, \dot{T}_e, t) + N_d(T_{ed}, \dot{T}_{ed}, t). \tag{24}$$

Remark 8 *It can be shown (see Appendix A) that $\tilde{N}(\cdot)$ defined in equation (22) can be upper bounded as follows*

$$\tilde{N} \leqslant \rho_N \|z\| \tag{25}$$

where $z(t) \in \mathbb{R}^2$ is defined as

$$z \triangleq [e \quad s]^T, \tag{26}$$

and $\rho_N \in \mathbb{R}^1$ is some positive constant. The inequality given by equation (25) will be utilized in the subsequent stability analysis.

[1] The second term in (18) is used to ensure that $u_1(t_0) = 0$.

Remark 9 *From the definition of $N_d(t)$ given by equation (23), and the explicit definition of $N(t)$ given in equation (12), the following expressions can be obtained*

$$N_d(t) = C_e \ddot{T}_{ed} - \dot{Q}_{in}, \tag{27}$$

$$\dot{N}_d(t) = C_e \dddot{T}_{ed} - \ddot{Q}_{in}$$

Clearly, from Remark 1, and Remark 4, $N_d(t)$, $\dot{N}_d(t) \in \mathcal{L}_\infty$.

To obtain the second closed loop error system, equation (19) is substituted in equation (15) to obtain

$$\begin{aligned} \dot{y} &= \left[\left(\frac{1}{C_e}+\frac{1}{C_r}\right)u_3(y+\varepsilon_1) - K_\eta \frac{1}{C_r}(T_r - T_\infty)\, u_3^2(y+\varepsilon_1)^2\right] \\ &\quad - \left[\frac{1}{C_e}(Q_{in}+Q_H) + \frac{1}{C_r}Q_0(t)\right] - K_e \frac{1}{C_r}(T_r - T_\infty)(y+\varepsilon_1)^2 \end{aligned} \tag{28}$$

5 Stability Analysis

To prove the stability of the closed-loop system, the closed loop system given in equation (28) is first upper bounded as

$$\dot{y} \le \left[\left(\frac{1}{C_e}+\frac{1}{C_r}\right)u_3(y+\varepsilon_1) - \varepsilon_0 K_\eta \frac{1}{C_r} u_3^2(y+\varepsilon_1)^2\right] - \varepsilon_0 K_e \frac{1}{C_r}(y+\varepsilon_1)^2 \tag{29}$$

where Remark 2 and Remark 3 have been used. After completing the square for the bracketed term, and expanding the squared term in the last term, in equation (29), it may be rewritten as

$$\dot{y} \le \alpha_1 - \alpha_2 y \tag{30}$$

where α_1 and $\alpha_2 \in \mathbb{R}^1$ are positive constants of analysis defined explicitly as

$$\alpha_1 = \frac{(C_e + C_r)^2}{\varepsilon_0 K_\eta C_e^2 C_r} \qquad \alpha_2 = \frac{2\varepsilon_1 \varepsilon_0 K_e}{C_r}. \tag{31}$$

From equation (30), the bound for $y(t)$ can be established as

$$y(t) \le y(0)\exp(-\alpha_2 t) + \frac{\alpha_2}{\alpha_1}\left[1 - \exp(-\alpha_2 t)\right]; \tag{32}$$

hence, $y(t) \in \mathcal{L}_\infty$. From Remark 7, it is clear that $\eta(t) \neq 0, \forall t \ge 0$.

Lemma 1 *Let the auxiliary function $L(t) \in \mathbb{R}$ be defined as follows*

$$L \triangleq s\left(N_d - \rho sgn(e)\right). \tag{33}$$

If the control gain ρ is selected to satisfy the following sufficient condition

$$\rho > |N_d(t)| + \frac{1}{\beta}\left|\dot{N}_d(t)\right|, \tag{34}$$

then

$$\int_{t_0}^{t} L(\tau)d\tau \leqslant \zeta_b \tag{35}$$

where the positive constant $\zeta_b \in \mathbb{R}^1$ is defined as

$$\zeta_b \triangleq \rho\,|e(t_0)| - e(t_0)N_d(t_0). \tag{36}$$

Proof. See Appendix B.

Theorem 2 *Provided that the control gain* ρ *is adjusted according to equation (34), the control law of equation (18) ensures that all system signals are bounded under closed-loop operation and that*

$$\lim_{t\to\infty} e(t),\ \dot{e}(t) = 0. \tag{37}$$

Proof. Let the auxiliary function $P(t) \in \mathbb{R}^1$ be defined as follows

$$P(t) \triangleq \zeta_b - \int_{t_0}^{t} L(\tau)d\tau \tag{38}$$

where ζ_b and $L(t)$ were defined in Lemma 1. It is easy to see that the use of Lemma 1 ensures $P(t) \geqslant 0$. Continuing with the proof, the function $V(t,x)$: $\mathbb{R}_+ \times \mathbb{R}^3 \to \mathbb{R}_+$ is defined as

$$V \triangleq \frac{1}{2}e^2 + \frac{1}{2}C_e s^2 + P \tag{39}$$

where $x(t) \in \mathbb{R}^3$ is defined as

$$x \triangleq [z^T \quad \sqrt{P}]^T \tag{40}$$

and $z(t)$ was defined in equation (26). Note that equation (39) can be bounded as

$$\lambda_1 \left\|x\right\|^2 \leq V \leq \lambda_2 \left\|x\right\|^2 \tag{41}$$

where λ_1, $\lambda_2 \in \mathbb{R}^1$ are defined as follows

$$\lambda_1 \triangleq \frac{1}{2}\min\{1, C_e\} \qquad \lambda_2 \triangleq \max\{1, C_e\}. \tag{42}$$

After taking the time derivative of equation (39) and substituting from equations (7) and (24), the expression obtained for $\dot{V}(t)$ is given by

$$\begin{aligned} \dot{V} &= -\beta e^2 - \beta s^2 + s\tilde{N} - k_s s^2 + s\left(N_d - \rho \operatorname{sgn}(e)\right) - L \\ &= -\beta e^2 - \beta s^2 + s\tilde{N} - k_s s^2 \end{aligned} \tag{43}$$

upon use of (33). After applying equations (25) and (26), the right-hand side of equation (43) can upper bounded as follows

$$\dot{V} \leq -\lambda_3 \left\|z\right\|^2 + \left[\rho_N \left|s\right| \left\|z\right\| - k_s \left|s\right|^2\right]. \tag{44}$$

After completing the squares on the bracketed term in equation (44), $\dot{V}(t)$ may be further upper bounded as

$$\dot{V} \leq -\gamma \left\|z\right\|^2. \tag{45}$$

where $\gamma \in \mathbb{R}^1$ is a positive constant that is defined as

$$\gamma = \lambda_3 - \frac{\rho_N^2}{4k_s}. \tag{46}$$

From (45), it is straightforward to see that $e(t)$, $s(t) \in \mathcal{L}_\infty$. From Remark 5, $\dot{e}(t) \in \mathcal{L}_\infty$. After taking the time derivative of equation (9) and using the system dynamics given in equation (1), the open loop expression for $\dot{e}(t)$ is obtained as

$$C_e\dot{e} = C_e\dot{T}_{ed} - Q_{in}(t) - u_1. \tag{47}$$

Using the previously made arguments, Remarks 1 and 4, and equation (20), it can be stated that $u_1(t)$, $\dot{u}_1(t) \in \mathcal{L}_\infty$. The fact that $\eta(t) \neq 0, \forall t \geq 0$ implies that $u_3(t) \in \mathcal{L}_\infty$. From the above facts and Remark 7, it is clear that $Q_H(t) \in \mathcal{L}_\infty$. From equation (19), it is easy to see that $u_2(t) \in \mathcal{L}_\infty$. Using Remark 4 and the prior facts, it can be seen that $T_e(t)$, $\dot{T}_e(t) \in \mathcal{L}_\infty$. In order to show that $T_r(t) \in \mathcal{L}_\infty$, the first time derivative of equation (10) is calculated and simplified as

$$\dot{\eta} = -\left[\left(\frac{1}{C_e} + \frac{1}{C_r}\right)u_3 + \frac{1}{C_r}u_2\right]\eta + \frac{1}{C_e}(Q_{in} + Q_H) + \frac{1}{C_r}Q_0(t) + \frac{1}{C_r}(T_e - T_\infty)u_2 \tag{48}$$

Standard arguments may be applied to equation (48) to prove that $\eta(t) \in \mathcal{L}_\infty$, since the first term within the brackets always remains positive (see Remark 7) and the second bracketed term is bounded based on previous arguments . Standard signal chasing arguments can now be used to show that the remaining signals in the system also remain bounded in closed loop operation. In particular, $\dot{e}(t)$, $\dot{s}(t) \in \mathcal{L}_\infty$. Equations (26) and (45) can also be utilized to show that $e(t)$, $s(t) \in \mathcal{L}_2$. After employing a corollary to Barbalat's Lemma [13], it is easy to show that (37) is valid. ■

6 Simulation Results

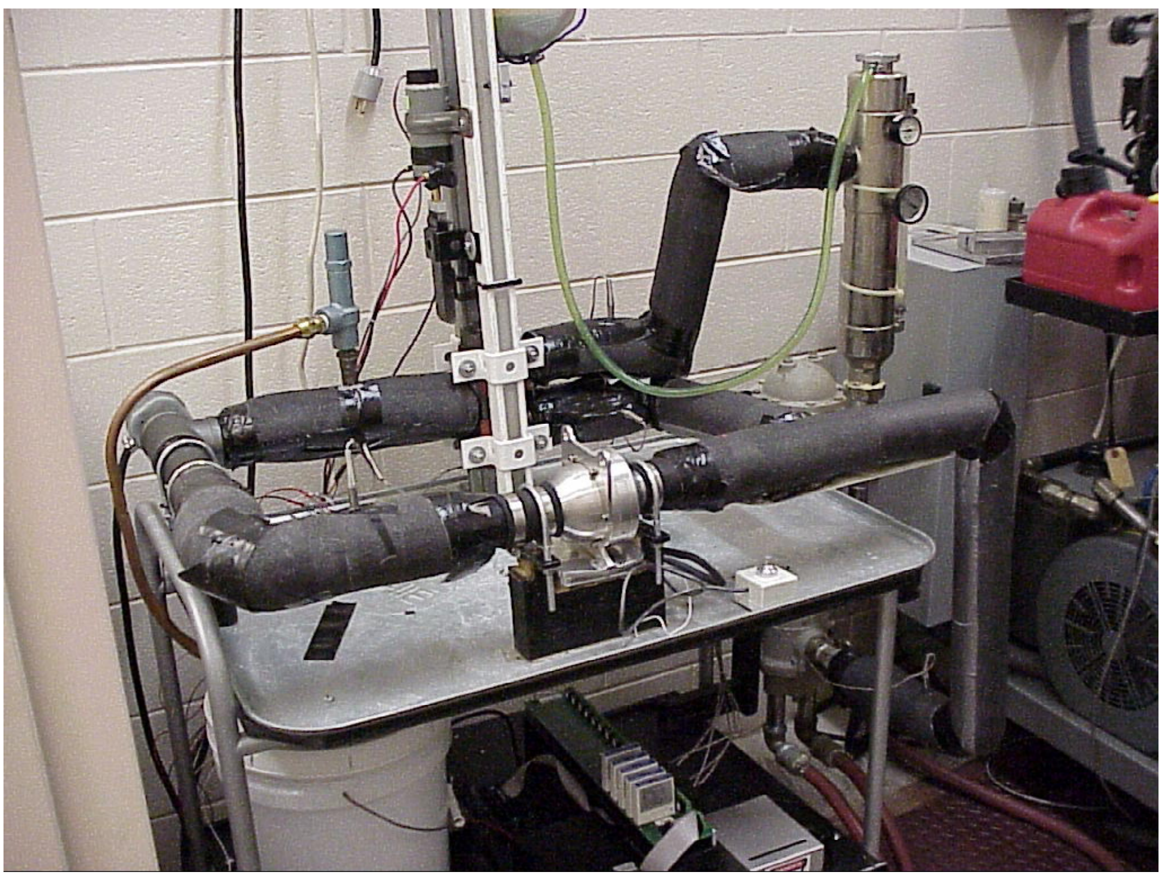

Figure 3: Scaled Automotive Thermal System Setup

The simulated scaled thermal system (See Figure 3) was assumed to have the model described by (1), (2), and (3). The unmeasurable heat from the engine, $Q_{in}(t)$ and the unmeasurable heat dissipated from the radiator, $Q_0(t)$, were chosen to be ([18])

$$Q_{in}(t) = 900\left(1+\cos\left(0.2t\right)\right)\ \text{W} \qquad \text{and} \qquad Q_0(t) = 50\left(1+\sin\left(0.1t\right)\right)\ \text{W} \tag{49}$$

respectively. The system parameters were chosen to be

$$\begin{array}{lllll} c_{pa} = 1107\ \text{J/kg}^o\text{K} & c_{pc} = 3098.2\ \text{J/kg}^o\text{K} & T_\infty = 293.15\ ^o\text{K} & r = 0.2\ \text{m} & \varepsilon = 0.8 \\ \rho_a = 1.177\ \text{kg}/m^3 & C_e = 100\ \text{J}/^o\text{K} & A = 1.435\ \text{m}^2 & C_r = 100\ \text{J}/^o\text{K} & \end{array} \tag{50}$$

The reference engine temperature trajectory was chosen to be

$$T_{ed} = 360 + 10\sin(0.1t)^o\text{K}$$

The temperatures of the engine and the radiator were initialized to be

$$T_e(0) = 360^o\text{K} \qquad T_r(0) = 303^o\text{K} \tag{51}$$

The control gains for the proposed control laws were chosen to be

$$K_s = 800 \quad \beta = 1 \quad \rho = 2500 \quad K_\eta = 0.01 \quad K_e = 1. \tag{52}$$

In Figure 4, the desired and actual engine temperatures are shown. The corresponding tracking error, $e(t)$, is shown in Figure 5. It is observed that the tracking error remains within 0.5^oK at all times. Figure 6 shows the engine and radiator temperatures. The corresponding control inputs required to achieve the control objective are shown in Figures 7 through 9.

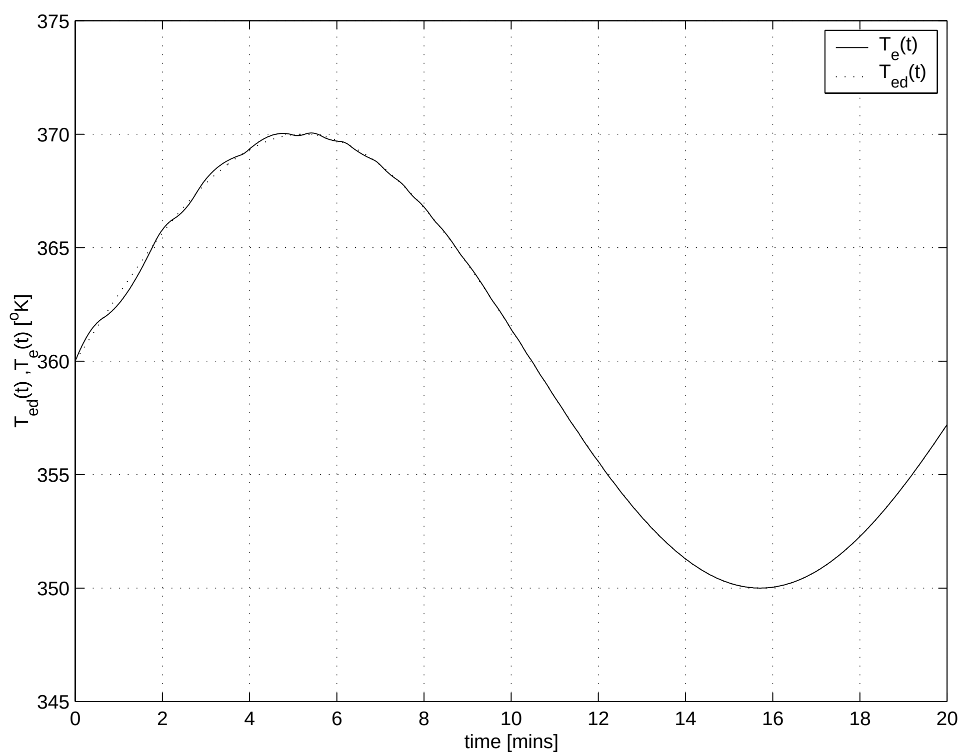

Figure 4: Desired and Actual Engine Temperatures ($T_{ed}(t)$, $T_e(t)$) in ^{o}K

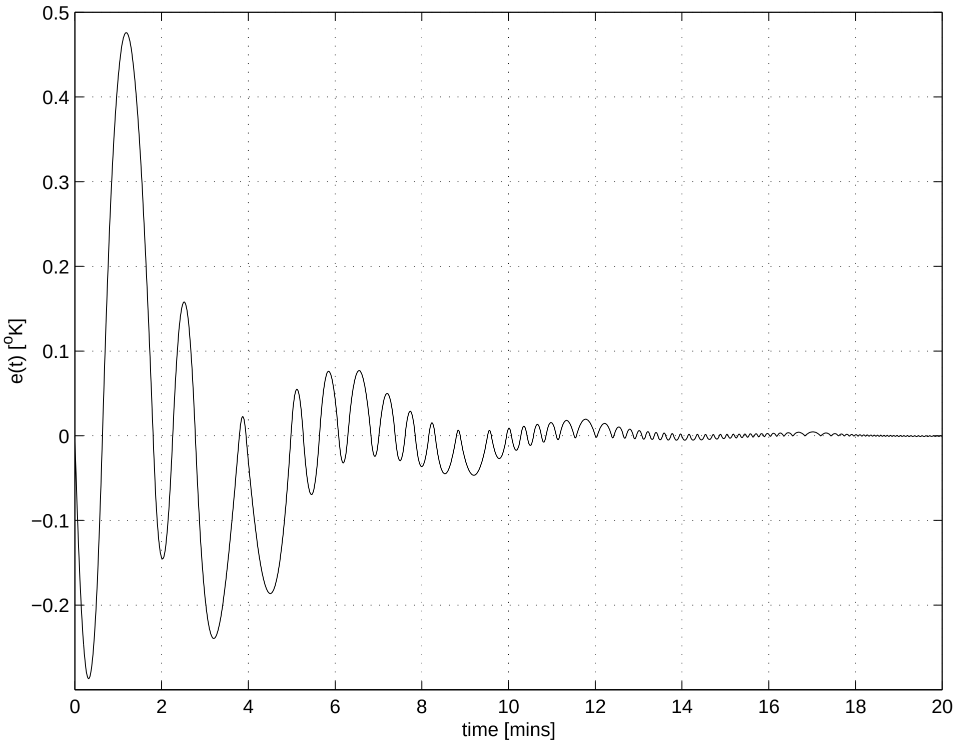

Figure 5: Engine Temperature Tracking Error ($e(t)$) in ^{o}K

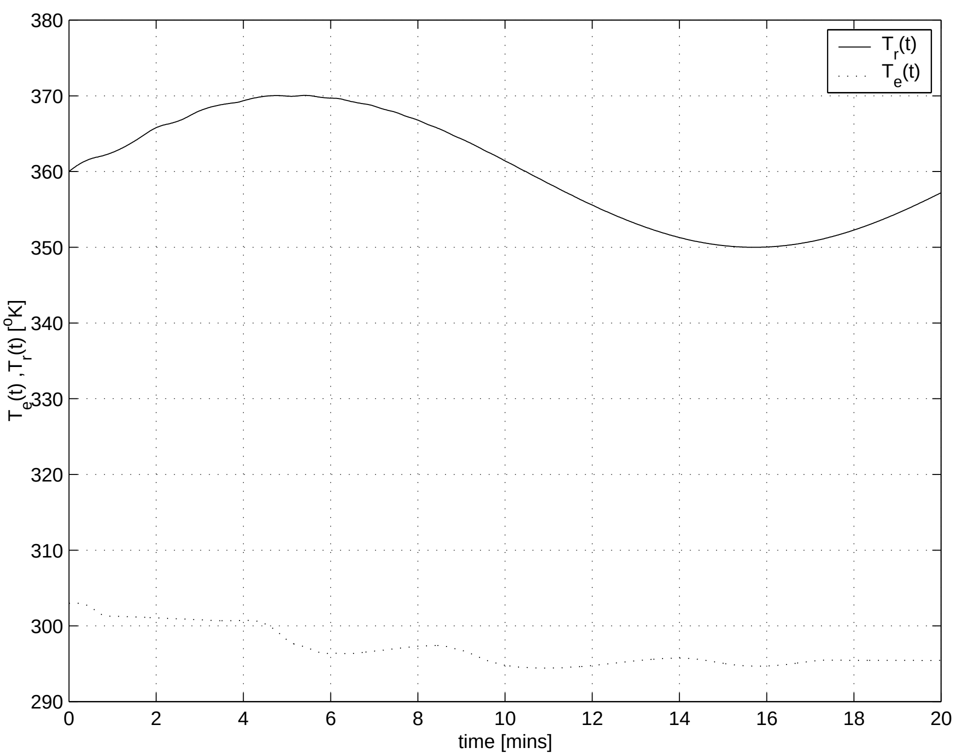

Figure 6: Engine and Radiator Temperatures ($T_e(t)$, $T_r(t)$) in ^{o}K

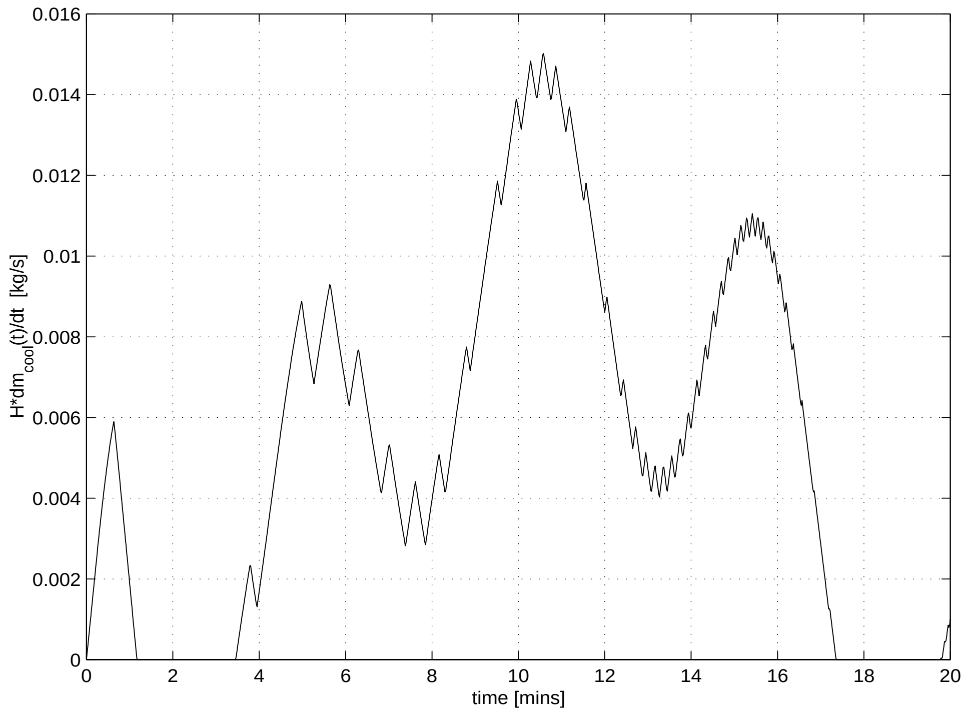

Figure 7: Coolant Flow Rate through Radiator ($H\dot{m}_{cool}$) in kg/s

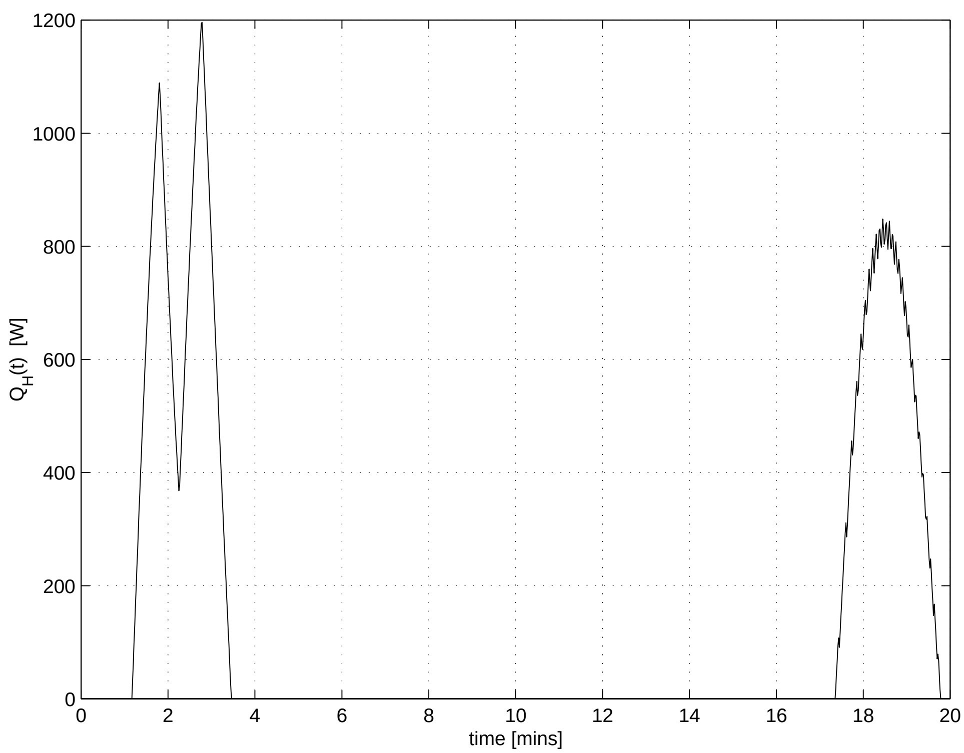

Figure 8: Heater Input ($Q_H(t)$) in W

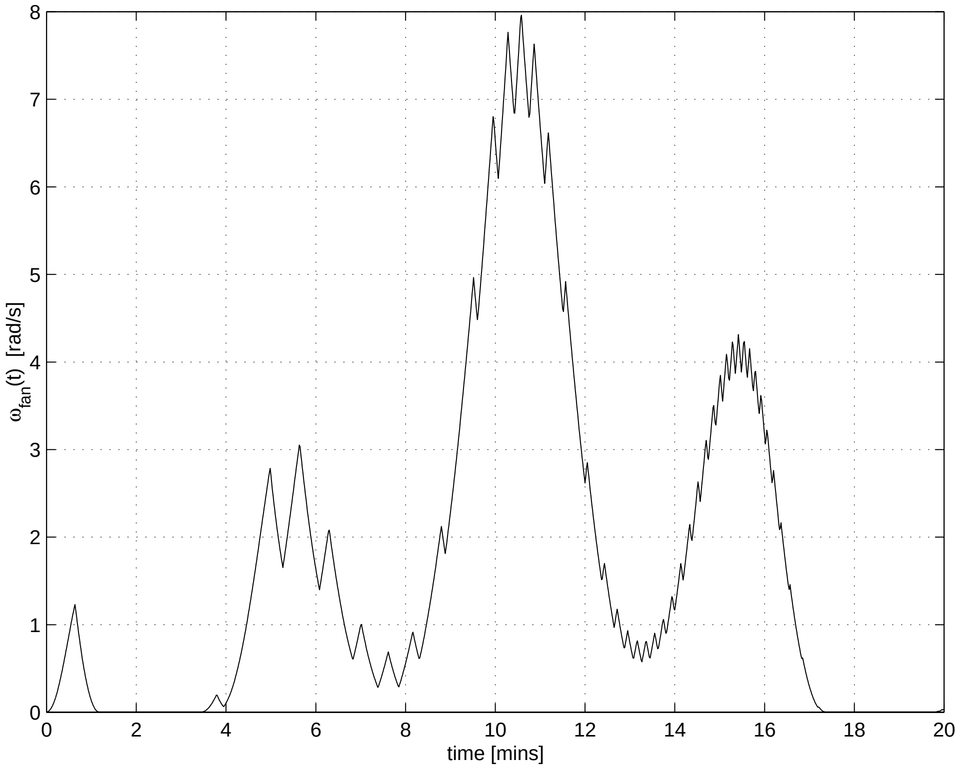

Figure 9: Roatational Speed of Radiator Fan ($\omega_{fan}(t)$) in rad/s

7 Conclusion

In this paper, the design of a nonlinear tracking controller has been presented which ensures that the engine temperature follows a desired temperature profile, and all signals remain bounded. A complete stability analysis, using Lyapunov-based techniques, has been presented to demonstrate that the proposed control law guarantees global asymptotic regulation of the engine temperature tracking error. Representative numerical simulation results have been presented to validate the performance of the proposed control law.

References

[1] Allen, D. A., and Lasecki, M. P., "Thermal Management Evolution and Controlled Coolant Flow", *SAE* paper no. 2001-01-1732, 2001.

[2] Barron, M. B., and Powers, W. F., "Role of Electronic Controls for Future Automotive Mechatronic Systems", *IEEE/ASME Transactions on Mechatronics*, vol. 1, no. 1, pp. 80-88, 1996.

[3] Chowanietz, E. G., "Automobile Electronics in the 1990s. Part 1: Powertrain Electronics", *Electronics and Communication Engineering Journal*, vol. 7, no. 1, pp. 23-36, 1995.

[4] Couetouse, H., and Gentile, D., "Cooling System Control in Automotive Engines", *SAE* paper no. 920788, 1992.

[5] Dawson, D., Hu, J., and Burg, T., *Nonlinear Control of Electric Machinery*, New York: Marcel Dekker, Inc., 1998.

[6] Einaudi, G., and Mortara, W., "Engine Cooling Electronic Control System", *SAE* paper no. 885085, 1988.

[7] Gunter, L. A., and Nalim, M. R., "Dynamic Performance of Conventional and Electrically Activated Engine Thermostats", *Proceedings of the ASME Internal Combustion Engine Division Conference*, Philadelphia, PA, April 2001.

[8] Hnatczuk, W., Lasecki, M. P., Bishop, J., and Goodell, J., "Parasitic Loss Reduction for 21st Century Trucks", *SAE* paper no. 2000-01-3423, 2000.

[9] Kenny, A. A., Bradshaw, C. F., and Creed, B. T., "Electronic Thermostat System for Automotive Engines", *SAE* paper no. 880265, 1988.

[10] Melzer, F., Hesse, U., Rocklage, G., and Schmitt, M., "Thermomanagement", *SAE* paper no. 1999-01-0238, 1999.

[11] Qu, Z., Xu, J., "Model Based Learning Controls and their Comparisons using Lyapunov Direct Method" *Asian Journal of Control, Special Issue on Learning Control,* Vol. 4, No.1, March 2002, accepted to appear.

[12] Setlur, P., Dawson, D., Chen, J., Wagner, J., "A Nonlinear Tracking Controller for a Haptic Interface Steer-by-wire systems", *Proceedings of the IEEE Conference on Decision and Control*, Las Vegas, NV, Dec. 2002, Accepted.

[13] Slotine, J. J. and Li, W. "Applied Nonlinear Control", Englewood Cliff, NJ: Prentice Hall, Inc., 1991.

[14] Visnic, B., "Thermostat, Thy Days are Numbered", *Wards AutoWorld*, vol. 37, no. 6, pp. 53-54, June 2001.

[15] Wagner, J. R., Marotta, E. E., and Paradis, I., "Thermal Modeling of Engine Components for Temperature Predictions and Fluid Flow Regulation", *SAE* paper no. 2001-01-1014, 2001.

[16] Wagner, J., Paradis, I., Marotta, E., and Dawson, D., "Enhanced Automotive Engine Cooling Systems - A Mechatronics Approach", *International Journal of Vehicle Design*, vol. 28, nos. 1/2/3, pp. 214-240, 2002a.

[17] Wagner, J. R., Ghone, M., Dawson, D., and Marotta, E. E., "Coolant Flow Control Strategies for Automotive Thermal Management Systems", *SAE* paper no. 2002-01-0713, 2002b.

[18] Wagner, J. R., Srinivasan, V., Dawson, D. M., and Marotta, E. E., "Smart Thermostat and Coolant Pump Control for Engine Thermal Management Systems", *SAE* paper, 2003, to appear.

[19] Xu, Z., Johnson, J. H., and Chiang, E. C., "A Simulation Study of a Computer Controlled Cooling System for a Diesel Powered Truck", *SAE* paper no. 841711, 1984a.

[20] Xu, Z., Johnson, J. H., and Chiang, E. C., "The Design and Testing of a Computer Controlled Cooling System for a Diesel Powered Truck", *SAE* paper no. 841712, 1984b.

A Appendix A

To simplify the following derivations, we start by rewriting (12) and (23) as follows

$$N(T_e, \dot{T}_e, t) = C_e \ddot{T}_{ed} - \dot{Q}_{in} + \beta \dot{e} + e \tag{53}$$

and

$$N_d = N(T_{ed}, \dot{T}_{ed}, t) = C_e \ddot{T}_{ed} - \dot{Q}_{in} \tag{54}$$

respectively. After substituting equations (53) and (54) in equation (22), the following expression is obtained for $\tilde{N}(t)$

$$\tilde{N} = \beta \dot{e} + e, \tag{55}$$

which may be upper bounded as

$$\tilde{N} \leq \beta |\dot{e}| + |e| \, . \tag{56}$$

Using the definition of $z(t)$ given in equation (26), $\tilde{N}(t)$ can be bounded as

$$\tilde{N} \leq \rho_N \, ||z|| \tag{57}$$

B Appendix B

After substituting (7) into (33) and then integrating in time, the following expression is obtained

$$\int_{t_0}^{t} L(\tau) d\tau = \int_{t_0}^{t} \beta e(\tau) \left(N_d(\tau) - \rho \mathrm{sgn}(e(\tau)) \right) d\tau + \int_{t_0}^{t} \frac{de(\tau)}{d\tau} N_d(\tau) d\tau - \rho \int_{t_0}^{t} \frac{de(\tau)}{d\tau} \mathrm{sgn}(e(\tau)) d\tau. \tag{58}$$

After integrating the second integral on the right-hand side of (58) by parts, equation (58) may be rewritten as

$$\begin{aligned} \int_{t_0}^{t} L(\tau) d\tau &= \int_{t_0}^{t} \beta e(\tau) \left(N_d(\tau) - \rho \mathrm{sgn}(e(\tau)) \right) d\tau + e(\tau) N_d(\tau)|_{t_0}^{t} - \int_{t_0}^{t} e(\tau) \frac{dN_d(\tau)}{d\tau} d\tau \\ &\quad - \rho \, |e(\tau)||_{t_0}^{t} \\ &= \int_{t_0}^{t} e(\tau) \left(\beta N_d(\tau) - \frac{dN_d(\tau)}{d\tau} - \beta \rho \mathrm{sgn}(e(\tau)) \right) d\tau + e(t) N_d(t) - e(t_0) N_d(t_0) \\ &\quad -\rho \, |e(t)| + \rho \, |e(t_0)| \, . \end{aligned} \tag{59}$$

The right-hand side of (59) may now be upper bound as follows

$$\begin{aligned} \int_{t_0}^{t} L(\tau) d\tau \;\leqslant\; & \int_{t_0}^{t} |e(\tau)| \left(\beta \, |N_d(\tau)| + \left| \frac{dN_d(\tau)}{d\tau} \right| - \beta \rho \right) d\tau + |e(t)| \left(|N_d(t)| - \rho \right) \\ & +\rho \, |e(t_0)| - e(t_0) N_d(t_0). \end{aligned} \tag{60}$$

From (60), it is easy to see that if ρ is chosen according to (34), then (35) holds.